

Planning of Electric Vehicle Charging Facilities on Highways Based on Chaos Cat Swarm Simulated Annealing Algorithm

Qingqiao GENG, Dongye SUN, Yuanhua JIA*

Abstract: Aiming at the layout planning of electric vehicle (EV) charging facilities on highways, this study builds a multi-objective optimization model with the minimum construction cost of charging facilities, minimum access cost to the grid, minimum operation and maintenance cost, and maximum carbon emission reduction benefit by combining the state of charge (SOC) variation characteristics and charging demand characteristics of EVs. A chaos cat swarm simulated annealing (CCSSA) algorithm is proposed. In this algorithm, chaotic logistic mapping is introduced into the cat swarm optimization (CSO) algorithm to satisfy the planning demand of EV charging facilities. The location information of the cat swarm is changed during iteration, the search mode and tracking mode are improved accordingly. The simulated annealing method is adopted for global optimization search to balance the whole swarm in terms of local and global search ability, thus obtaining the optimal distribution strategy of charging facilities. The case of the Xi'an highway network in Shanxi Province, China, shows that the optimization model considering carbon emission reduction benefits can minimize the comprehensive cost and balance economic and environmental benefits. The facility spacing of the obtained layout scheme can meet the daily charging demand of the target road network area.

Keywords: chaos cat swarm simulated annealing algorithm; charging facility planning; electric vehicle; highway; simulated annealing method

1 INTRODUCTION

As a significant way to alleviate the energy crisis and environmental pollution, electric vehicles (EVs) have been vigorously developed in recent years [1-3]. By the end of 2021, there were 1.14 million public charging infrastructures in China, with public fast-charging and slow-charging piles reaching 85% and 55% of the global share, respectively. The total number of charging piles reached 2.61 million, with 1.47 million private charging piles and a comprehensive vehicle-pile ratio of 3:1. Compared with the static demand from fixed points or areas, the charging demand of EVs on highways is mainly a dynamic demand of passing on the traffic network [4, 5]. This demand is mainly for EVs that are in long-term mobility during long-distance driving, and their charging demand mostly arises during driving [6, 7]. Therefore, it is of great theoretical significance and application value to ensure sufficient power supply for EVs when driving on highways according to the distribution of charging demand and to reasonably select the location of charging facilities by combining constraints such as traffic road network and distribution network [8, 9]. In this way, planning objectives such as charging convenience and economy for EV users and revenue for charging operators can be optimized [10].

The layout planning for EV charging facilities is mainly based on facility planning by combining optimization objectives and constraints of each participating subject in the use phase. A charging facility location model can be used to select suitable locations for the construction of charging stations in the proposed planning area [11, 12]. A reasonable capacity design can minimize the related costs and maximize the operating revenue and charging demand while satisfying the multiple constraints of charging participating subjects [13]. The widely used models for charging facility siting include the p-center model, p-median model, coverage model, network equilibrium model and interception model [14-16]. The determination of capacity needs to consider various factors, such as space constraints of charging facilities and charging cost constraints. The commonly used methods to determine capacity include the probability prediction

method, flowmeter algorithm and queuing theory [17]. In summary, existing studies mainly focus on the planning of EV charging facilities in urban areas, with less research on the planning of highway charging facilities [18]. Additionally, the planning layout is mainly based on the division of service areas, with less consideration of the influence of traffic factors. The location and capacity of charging facilities are separated without considering their mutual influence [19]. Moreover, most existing studies only consider the construction and operation costs of charging facilities or charging convenience [20]. The optimization objectives and constraints involved are relatively single, and the planning model obtained is difficult to meet the needs and interests of all participants, such as EV users and construction operators [21, 22].

In terms of algorithm application, solutions to charging facility planning problems can be divided into the exact solution method and heuristic algorithm [23]. The former is mainly used for the exact solution of small optimization problems and includes the branch-and-bound method and decomposition method [24]. When the number of nodes and decision variables increases, the complexity of the problem will rise significantly, and the time cost of the actual exact solution will become unacceptable. Therefore, the application of the exact solution method in solving large optimization problems has certain limitations [25]. In contrast, the heuristic algorithm is mainly applied to solve large optimization problems in actual environments and can provide load requirements within an acceptable time frame [26, 27]. The heuristic algorithm includes the genetic algorithm (GA), particle swarm optimum algorithm, simulated annealing algorithm, greedy algorithm, and hybrid heuristic algorithm with two or more heuristics [28-30]. However, the above algorithms have limitations such as long-time consumption, poor stability, slow convergence, and sensitivity of algorithm performance to initial values and parameter settings [31].

The cat swarm optimization (CSO) algorithm is a new bionic algorithm that can search for the global optimal solution in a short time and converge fast by observing the daily behavior pattern of cats [32]. In this algorithm, the behavior pattern is divided into the tracking mode and the searching mode; the tracking process of cats is simulated

to search for the global optimal solution, and the local optimal solution is determined through the searching process of cats. The algorithm has a simple principle and few parameters, which is suitable for planning the distribution of EV charging facilities on highways with simple routes. However, with iteration, the search efficiency of the CSO algorithm gradually decreases, and the search accuracy improves slowly [33]. It is easy to fall into the local optimum, resulting in low tracking accuracy of the optimal value [34].

To address the limitations of the existing research on the layout planning of EV charging facilities in model algorithms, this study builds a multi-objective optimization model with the minimum construction cost of charging facilities, minimum access cost to the grid, minimum operation and maintenance cost, and maximum carbon emission reduction benefit by combining the state of charge (SOC) variation characteristics and charging demand characteristics of EVs. On this basis, a chaos cat swarm simulated annealing (CCSSA) algorithm is proposed. In this algorithm, chaotic logistic mapping is introduced into the CSO algorithm to satisfy the planning demand of EV charging facilities. The location information of the cat swarm is changed in the iterative process, and the search and tracking modes are improved accordingly. The method of copying a fixed number of cat copies is used in the search mode to prolong the convergence time, while the inertia weights are redefined according to the search speed in the tracking mode. The global search for superiority is conducted by simulated annealing to balance the whole swarm in terms of local and global search ability, thus obtaining the optimal distribution strategy of charging facilities. Moreover, the effectiveness and superiority of the proposed model and algorithm are verified in the case of the highway network in Xi'an, Shanxi Province, China. The result provides a reference for the layout planning of EV charging facilities and low-carbon highway construction.

The rest of this paper is arranged as follows. Firstly, the charging demand for EVs is analyzed in Section 2. Section 3 presents the framework structure and each constraint of the layout planning model for charging facilities. Section 4 provides the main steps of the CCSSA algorithm solution. In Section 5, the effectiveness of the proposed approach is verified by analyzing the arithmetic examples of the actual highway network. Finally, conclusions and future research directions are shown in Section 6.

2 CHARGING DEMAND ANALYSIS

The EV has the characteristics of SOC decreasing with the increase in driving distance. When driving on the highway, EVs face great power consumption and frequent charging demand [4]. For a single highway, there are vehicles at the entrance and exit, and EV charging stations are built on both sides of the highway. Charging stations on both sides do not affect each other since vehicles on the highway drive in one direction, and the traffic flow in both directions does not affect each other [21]. In addition, EVs have an initial SOC when entering the highway at a certain moment and need to meet a certain SOC retention S_{res} when leaving from the exit to ensure subsequent normal driving. Then, when the initial electric energy retention is S_0 , and the driving path and the distribution of charging stations

are known, the SOC of EVs at any location on the highway can be obtained:

$$S_i = f(L_i) \tag{1}$$

where S_i is the SOC of the EV at point i , and L_i is the position of the i th EV on the highway. Specifically, the SOC of the EV at any point is the initial power minus the consumed power plus the charging power:

$$S_i = S_0 - \frac{D_i \beta_i}{C_i} + \sum_{k=1}^{N_c} y_k z_{i,k} (S_{up} - S_{i,k}) \tag{2}$$

where D_i is the distance traveled by the i -th EV; β_i is the power consumption per unit mile of the i -th EV; C_i is the battery capacity of the i -th EV; N_c is the number of candidate station sites in the road network; S_{up} is the SOC of the EV after charging; $y_k = 1$, if the station is built at the candidate station site at point k in the road network, and 0 otherwise; $z_{i,k}$ indicates whether the i -th EV chooses to charge when it passes by the charging station at point k ; $z_{i,k} = 1$, if charging, and $z_{i,k} = 0$, if not charging; $S_{i,k}$ is the SOC of the i -th EV when it passes by the charging station at point k .

Based on the SOC calculation of EVs on a single highway, the SOC distribution of the whole road network can be obtained by superimposing the SOC changes of each vehicle. For any point in the road network, n EVs pass by in period t . The SOC of each EV passing by the point can be obtained by Eq. (2). After counting the SOC of the vehicles passing in period t and calculating the power required by the EVs whose SOC is in the rechargeable interval $[0, S_{down})$, the EV charging demand $Q_{t,k}$ at point k in period t can be obtained:

$$Q_{t,k} = \sum_{i=1}^{n_{t,k}} z_{i,k} (S_{up} - S_{i,k}) C_i \tag{3}$$

where $n_{t,k}$ is the number of EVs at point k in period t . By integrating all periods throughout the day, the EV charging demand $Q_{T,k}$ at point k of the highway network within one day can be obtained:

$$Q_{T,k} = \sum_{t \in T} Q_{t,k} \tag{4}$$

where T is the set of all periods throughout the day. The total charging demand can be expressed by the driving distance of EVs. With a known power consumption per unit path, assuming that the initial electric quantity S_0 when an EV arrives at the road network follows the normal distribution, and the average remaining power when the EV leaves the road network is S_{left} , the total charging power of EVs in the whole road network can be expressed as:

$$Q_{sum} = \sum_{i=1}^{n_T} [S_{i,total} \beta_i + (S_{left} - S_0) C_i] \tag{5}$$

where $S_{i,total}$ is the total distance traveled by the i -th vehicle, and n_T is the total number of EVs passing by the road network in period T .

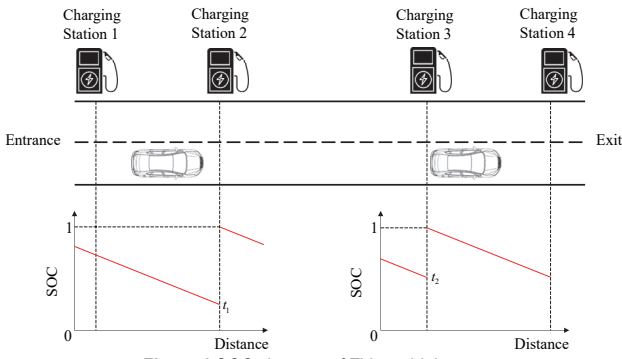


Figure 1 SOC changes of EVs on highways

3 PLANNING MODEL OF CHARGING FACILITIES

3.1 Objective Function

Considering the construction, operation, maintenance characteristics of EV charging stations, we build a multi-objective optimization model with the minimum construction cost of charging facilities, minimum access cost to the grid, minimum operation and maintenance cost, and maximum carbon emission reduction benefit for low-carbon construction of highways:

$$\min C = \delta [c_{EVCS}(Y, N) + c_{S2G}(Y, N) + c_{oper}(Y, N) - c_{emi}(Y, N)] \quad (6)$$

$$\delta = (A/P, i, s) = \frac{i(1+i)^s}{(1+i)^s - 1} \quad (7)$$

where C is the annual average comprehensive cost of constructing a charging station; Y is the decision variable for constructing a charging station; N is the decision variable of the number of charging machines (indicating charging capacity) in the charging station; δ is the capital recovery coefficient, representing the equivalence relationship between the known present value P and s equal annual values A ; i is the discount rate. The objective function contains four parts. The first component is the construction cost $c_{EVCS}(Y, N)$ of the charging station, including fixed cost $c_{fix}(Y, N)$ associated with whether to construct a station and variable cost $c_{var}(Y, N)$ associated with station capacity.

$$c_{EVCS}(Y, N) = c_{fix}(Y, N) + c_{var}(Y, N) \quad (8)$$

$$c_{fix}(Y, N) = \sum_{k=1}^{N_c} y_k c_{cs,k} \quad (9)$$

$$c_{var}(Y, N) = \sum_{k=1}^{N_c} (N_k c_{ch} + c_{tr} S_k^{ET}) \quad (10)$$

$$S_k^{ET} = \frac{N_k K_{ch} P_{ch}}{L_{max} \alpha_{cs} \eta_{ch} \cos \phi_{ch}} \quad (11)$$

where $c_{cs,k}$ is the fixed cost of the charging station at point k ; $y_k = 1$ if the station is built at point k , and $y_k = 0$ if no station is built; S_k^{ET} is the transformer capacity of the charging station at point k ; N_k is the number of chargers; c_{ch}

is the cost of a single charger; c_{tr} is the cost of distribution equipment (such as transformers and switches) per unit capacity; P_{ch} is the rated output power of a single charger; K_{ch} is the simultaneous charging rate; η_{ch} is the efficiency of the charger; $\cos \phi_{ch}$ denotes the power factor of the charger; L_{max} is the maximum daily load factor of the charging station; α_{cs} is the ratio of the charging load to the total load for the charging station.

The construction of charging stations on highways requires electrical power from nearby substations. According to the proximity principle [35], it can be assumed to connect from the nearest substation if the load factor requirements are met. Therefore, the total cost includes the cost of connection to the grid, i.e., the second part of the objective function is:

$$c_{S2G}(Y, N) = \sum_{k=1}^{N_c} y_k c_{con} d_k K_{line} \quad (12)$$

where c_{con} is the engineering cost per km of 10 kV overhead lines; d_k is the distance from charging station k to the nearest charging station; K_{line} is the adjustment factor to avoid repeated investment in multiple lines. Charging stations require maintenance during operation. Thus, the third part of the objective function is the operation and maintenance cost $c_{oper}(Y, N)$, includes the electricity cost of stations c_{cs} , the labor cost c_{hr} related to the scale of charging stations, and the maintenance cost c_m :

$$c_{oper}(Y, N) = c_{cs} + c_{hr} + c_m \quad (13)$$

$$c_{cs} = c_p^* \sum_{k=1}^{N_c} y_k P_{cs}^{av} T_{cs}^{av} \quad (14)$$

$$c_{hr} = \sum_{k=1}^{N_c} c_{hr}^0 N_k \quad (15)$$

$$c_m = \sum_{k=1}^{N_c} c_m^0 S_k^{ET} \quad (16)$$

where c_p^* is the electricity price; p_{cs}^{av} is the average load of a charging station excluding charging equipment; T_{cs}^{av} is the average equivalent working time of a charging station each year; c_{hr}^0 is the average annual unit labor cost per charger of a charging station, c_m^0 is the average annual management cost of the unit transformer capacity of a charging station. The CO₂ emission reduction benefit of EVs relative to fuel vehicles is also an important part to be considered in the target cost function. Thus, the annual carbon emission benefit in the fourth part of the target function is:

$$c_{emi} = \sum_{k=1}^{N_c} d_m \sum_{t=1}^{24} \left[\sum_{i=1}^{n_{EV}} \frac{P_{i,t,EV}}{M_{EV}} \rho \Delta \right] \quad (17)$$

where M_{EV} is the electricity consumption of EVs per 100 km; d_m is the number of days in each season; ρ is the carbon emissions converted into an economic trading price; Δ is the reduction in CO₂ emissions of an EV relative to a fuel vehicle traveling 100 km.

3.2 Constraints

3.2.1 Number Constraints of Charging Stations

According to the planning requirements, the number of charging stations to be built is generally definite or within a certain range, i.e., between the minimum value N_{EVCS}^{\min} and the maximum value N_{EVCS}^{\max} :

$$N_{EVCS}^{\min} \leq \sum_{k=1}^{N_c} y_k \leq N_{EVCS}^{\max} \quad (18)$$

3.2.2 Capacity Constraints of Charging Stations

Affected by geographical location, surrounding environment, grid line capacity and planning requirements, the capacity of each charging station needs to meet certain constraints, i.e., the number of chargers needs to meet the following constraints:

$$N_k^{\min} \leq N_k \leq N_k^{\max} \quad k = 1, 2, \dots, N_c \quad (19)$$

3.2.3 Constraints of Charging Demand

For the overall planning of charging facilities, the interaction between all the stations to be built in the road network should be considered in calculating charging demand. The impact of charging station j on the charging demand at point k is divided into two cases. One case is that EVs charge at station j before point k , which reduces the charging demand at point k and is related to the traffic flow from j to k . The other case is the reduction of charging demand at station k due to the expectation of charging at station j after point k , which is related to the traffic flow from station k to j . Then, the charging demand at point k in period T can be expressed as:

$$Q_k^{cs} = \beta_k^{cs} \sum_{i=1}^{n_k} [(S_{up} - S_{i,0})B_i + D_{i,k}\sigma_i] - \sum_{j=1}^{N_c} y_j (\gamma_{jk}\rho_{jk} + \lambda_{jk}\rho_{jk})\Delta S_j^{av} B^{av} \quad (20)$$

where assuming that $\rho_{kj} = 0$ when $j = k$, n_k is the number of EVs passing by point k ; β_k^{cs} is the proportion of EVs charging at point k ; $D_{i,k}$ is the travel distance of the i -th EV from the highway entrance to point k ; ΔS_j^{av} is the average increase in SOC by charging at station j ; B^{av} is the average battery capacity of multiple EVs; γ_{jk} and λ_{jk} are the impact factors between charging stations; for charging stations after station k , it is considered that only stations within K_1 times the range affect station k ; S^{av} is the average range of EVs. The definition is as follows:

$$\begin{cases} \lambda_{kj} > 0, l_{jk} \leq K_1 S^{av} \\ \lambda_{kj} = 0, l_{jk} > K_1 S^{av} \end{cases} \quad (21)$$

The values of γ_{jk} and λ_{jk} depend on the service capacity of EV charging stations and the user's choice of charging timing. Assuming that the user of an EV traveling on a highway chooses to charge at least once per m charging station, each charging station serves $1/m$ of the traffic volume on the highway. Then, we can set $\gamma_{jk} = \lambda_{jk} = 1/m$. The first part on the right side of Equation (20) is the charging demand caused by EV driving loss and charging at point k , and the second part is the effect of other stations to be built on the charging demand at point k . The two parts can be subtracted to obtain the EV charging demand in one day at point k , and the corresponding constraint is:

$$Q_{cs}^k \leq \frac{N_k K_{ch} P_{ch} T_{cs}^{av}}{365} \quad (22)$$

3.2.4 Constraints of Charging Distance

To ensure the economy of charging station planning and satisfy the charging demand, the distance between two adjacent charging stations on the same path should not be too small or too large. It is assumed that the distance is not less than K_2 times the average range and not greater than K_3 times the average range:

$$K_2 S^{av} \leq l_{jk} \leq K_3 S^{av} \quad (23)$$

where l_{jk} is the distance between two adjacent candidate station sites j and k .

3.2.5 Logical Constraints of Variables

There is a logical constraint between the capacity of charging stations and station construction. If $y_k = 0$, station capacity $N_k = 0$; if $y_k = 1$, station capacity $N_k > 0$:

$$\begin{cases} -My_k + N_k \leq 0 \\ y_k - N_k \leq 0 \end{cases} \quad (24)$$

where M is a sufficiently large real number, and the decision variables Y and N belong to 0-1 variables and non-negative integer variables, i.e., $y_k \in \{0,1\}$, $N_k \in N$ and $N_k \geq 0$.

3.3 Mathematical model

Based on the analysis of the objective function and constraints, the optimal layout model of charging facilities in the highway network can be summarized as follows:

$$\begin{cases} \min C = f(x) \\ \text{s.t. } A_{ineq} \leq b_{ineq} \\ l_b \leq x \leq u_b; y_k \in \{0,1\}; N_k \geq 0 \end{cases} \quad (25)$$

where $f(x)$ is the objective function; x consists of Y and N and is the decision variable for the construction of EV charging stations. The constraints include inequality constraints and upper and lower bound constraints.

4 OPTIMIZATION ALGORITHM

The optimization model considering economic cost and carbon reduction benefits, has a relatively complex coupling relationship between decision variables and a higher solution space dimension, which is suitable for heuristic algorithms with fast local search speed, strong search ability and few adjustable parameters. As a heuristic algorithm, the CSO algorithm has strong portability of its coding rules, it has a good theoretical match with the layout optimization model constructed in this study, which can search for the global optimal solution in a short time. Besides, it is very suitable for layout planning of EV charging facilities on highways with clear lines. However, with the gradual increase of the number of iterations, the search efficiency of the CSO algorithm tends to decrease, the search accuracy improves slowly, and it is easy to mature prematurely [33]. Therefore, based on the planning model of EV charging facilities on the highway, this study proposes a CCSSA algorithm to optimize the layout of charging facilities. Chaotic logistic mapping is introduced into the CSO algorithm to change the location information of the cat swarm during iteration. The global optimization search is performed by the simulated annealing method to balance the whole swarm in terms of local and global search ability, thus obtaining the optimal layout of charging facilities. The relationship between the CCSSA algorithm and EV charging facility planning is shown in Fig. 2.

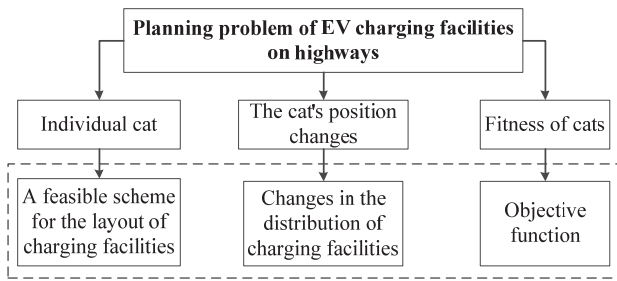


Figure 2 Relationship between the CCSSA algorithm and EV charging facility layout

The expression of a chaotic variable with a chaotic property is:

$$x(n+1) = ux(n)[1 - x(n)], n = 1, 2, \dots, N \tag{26}$$

where n is the number of iterations, and u is the chaos control parameter. When $u = 4$, $x \in [0, 1]$ and $x \notin [0.25, 0.50, 0.75]$, the system is in a fully chaotic state. When the conventional variables $Cx \in [a, b]$, the expression of the mapping transformation with chaotic variables is:

$$x(n) = [Cx(n) - a] / (b - a), n = 1, 2, \dots, N \tag{27}$$

$$Cx(n) = a + x(n)(b - a), n = 1, 2, \dots, N \tag{28}$$

where $Cx(n)$ represents the location variable of the cat

swarm, and $[a, b]$ is the traversal range of the cat swarm location. After the introduction of the logistic chaos sequence and simulated annealing method, the optimal value accuracy of the CSO algorithm was significantly improved, and the convergence time was shortened. To further improve the finding efficiency of the optimal value, the two modes of the CSO algorithm are improved as follows for the planning demand of EV charging facilities: in the search mode, the method variation of copying a fixed number of cat copies is used to extend the convergence time; in the tracking mode, the inertia weight $w = 1$ is set to completely inherit the current velocity. The specific flow of the CCSSA algorithm is as follows:

Step 1: The cat swarm is initialized, the swarm size of the CCSSA algorithm is set to N , and the maximum number of iterations k_{max} and the mixture ratio (MR) are set. The cat swarm location, velocity and related parameters are randomly initialized.

Step 2: The individual fitness of each cat is evaluated, the fitness value is calculated, and the best location fitness value is stored in P_{best} .

Step 3: The cats are randomly grouped according to the MR value, where MR represents the proportion of cats performing the tracking mode in the whole cat swarm, i.e., the proportion of feasible solutions for charging facilities in the whole charging facility layout. The MR value is generally small to ensure that most cats are in the search mode and a few are in the tracking mode.

Step 4: The initial temperature T_0 is determined, and the fitness value $TF(x_i)$ of each individual at the current temperature is determined:

$$T_0 = \frac{P_{best}}{\ln 5} \tag{29}$$

$$TF(x_i) = \frac{e^{-[f(x_i) - f(p_{best})]/n}}{\sum_{i=1}^N e^{-[f(x_i) - f(p_{best})]/n}} \tag{30}$$

Step 5: The search mode is optimized. Cat individuals are duplicated and deposited into the seeking memory pool (SMP). The number of duplicated cat individuals is determined by the size of their fitness values. A larger fitness value leads to a larger number of duplicated individuals. The formula for duplicated individuals is as follows:

$$N_i = fitness_i / (\sum_{i=1}^N fitness_i) N_{sum} \tag{31}$$

where N_i is the number of duplicated individuals of the i -th cat, N_{sum} is the total number of duplicated individuals, $fitness_i$ represents the fitness value of the i -th cat, and N is the initialized swarm size. The variation operator is executed, i.e., a random perturbation is applied to replace the original location with a new location, the SMP is updated, and the fitness values of all individuals are calculated. The selection operator is executed, i.e., the current cat location is replaced by calculating the candidate charging location with the highest fitness value in the SMP, and the EV charging facility layout is updated.

Step 6: The tracking mode is optimized. The roulette strategy is adopted to determine the best locations experienced by all cats, i.e., the best alternative value of each charging facility location. The optimal solution searched so far is let to $X_{best}(n)$, and the speed of each cat is let to V_i . Then, the updated speed value of the i -th cat is:

$$V_i(n+1) = V_i(n)w + rand[X_{best}(n) - V_i(n)]c \tag{32}$$

$$w = w_{max} - (w_{max} - w_{min})(k / k_{max}) \tag{33}$$

where w is the inertia weight, k is the iteration index, k_{max} is the maximum number of iterations, c is a constant, and $rand$ is a random number between 0 and 1. Then, the updated position of the i -th cat is:

$$X_i(n+1) = X_i(n) + V_i(n+1) \tag{34}$$

Step 7: The fitness value is calculated, the optimal fitness value in the swarm is recorded and kept, and whether the termination condition is satisfied is judged. If it is satisfied, the optimal solution is output, and the program is ended; otherwise, the mapping transformation is performed on the regular variable $C_x(n)$. After the mapping transformation, the chaotic variable $x(n)$ is between 0 and 1. The chaotic mapping is performed on the chaotic variable $x(n)$ to obtain $x(n+1)$, and then the mapping transformation is performed on the chaotic variable $x(n+1)$ to obtain the conventional variable $C_x(n+1)$ in the next iteration. Steps 2-7 are repeated for the optimization seeking

Step 8: The cooling operation is performed as follows:

$$T_{k+1} = \lambda T_k \tag{35}$$

where $\lambda \in [0.5, 1]$ is the cooling factor. If the exit condition is met, then the search stops, and the result is output; otherwise, Step 4 is entered. The solution calculation flow of the algorithm is shown in Fig. 3.

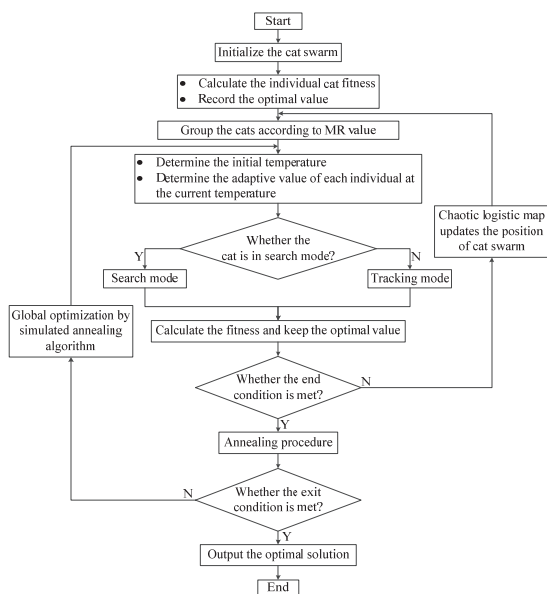


Figure 3 Flowchart of the CCSSA algorithm

5 EXAMPLE ANALYSIS

The road network structure used for the planning of highway charging facilities is shown in Figure 4. Taking the highway network in Xi'an City, Shaanxi Province, China, as an example, the calculation diagram of the road network shown in Fig. 5 was obtained. As shown in Fig. 5, there are 10 highway toll stations, 7 intersections, and 17 nodes and sections. The lengths of sections 1 to 17 are shown in Tab. 1. With the consideration of the two-way driving characteristics of the highway, the number of paths for EVs is 90, and there are two paths with opposite directions between every two entrances and exits. Based on the principle of the shortest circuit, the path between every two entrances and exits is uniquely determined. The distribution of origin and destination (OD) points of EVs between the entrances and exits of the highway network is shown in Tab. 2.

Table 1 Length of each section of the highway network

| Section number | Length / km | Section number | Length / km | Section number | Length / km |
|----------------|-------------|----------------|-------------|----------------|-------------|
| #1 | 25 | #7 | 26 | #13 | 32 |
| #2 | 31 | #8 | 17 | #14 | 31 |
| #3 | 35 | #9 | 22 | #15 | 42 |
| #4 | 27 | #10 | 24 | #16 | 41 |
| #5 | 21 | #11 | 22 | #17 | 43 |
| #6 | 33 | #12 | 16 | — | — |



Figure 4 Schematic diagram of the highway network

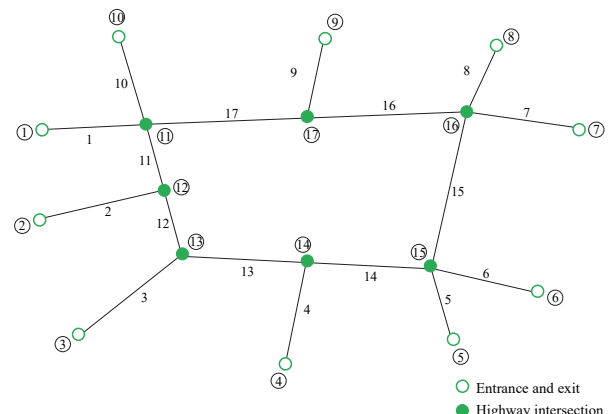


Figure 5 Simplified structure of the highway network

Table 2 Distribution of the OD points in the highway network

| Entrance | Exit | | | | | | | | | |
|----------|------|------|------|------|------|------|------|------|------|------|
| | 1 | 2 | 3 | 4 | 5 | 6 | 7 | 8 | 9 | 10 |
| 1 | 0 | 1254 | 1301 | 2224 | 1247 | 2313 | 1238 | 1292 | 1328 | 1351 |
| 2 | 1285 | 0 | 1189 | 1161 | 1224 | 1278 | 1326 | 1334 | 1245 | 1194 |
| 3 | 1323 | 1295 | 0 | 1224 | 2271 | 1289 | 1293 | 1315 | 1264 | 1288 |
| 4 | 2247 | 2203 | 1233 | 0 | 1235 | 1279 | 1313 | 1287 | 1246 | 1215 |
| 5 | 1251 | 1244 | 2308 | 1267 | 0 | 1263 | 1282 | 1293 | 1235 | 1259 |
| 6 | 2363 | 1256 | 1246 | 1324 | 1285 | 0 | 214 | 2265 | 1287 | 1322 |
| 7 | 1272 | 1290 | 1326 | 1345 | 1324 | 1226 | 0 | 1218 | 1265 | 1283 |
| 8 | 1339 | 1387 | 1347 | 1311 | 1319 | 1279 | 1247 | 0 | 1275 | 1303 |
| 9 | 1360 | 1209 | 1285 | 1273 | 1288 | 1312 | 1295 | 1293 | 0 | 1256 |
| 10 | 1399 | 1255 | 1316 | 1297 | 1278 | 1347 | 1330 | 1337 | 1289 | 0 |

5.1 Parameter Setting

According to the distribution characteristics in Tab. 2, six typical EVs were adopted for simulation calculation in this study. The battery capacities and driving ranges of the EVs are shown in Tab. 3.

Table 3 Parameters of the six classical EVs

| Vehicle type | Battery Capacity / kWh | Driving Range / km | Proportion / % |
|---------------|------------------------|--------------------|----------------|
| Tesla-Model3 | 80.0 | 470 | 28.44 |
| Nissan Leaf | 45.5 | 410 | 13.35 |
| Zotye-5008EV | 32.0 | 380 | 11.12 |
| Roewe-E50 | 38.8 | 290 | 12.39 |
| BJ-E150 | 26.5 | 360 | 13.03 |
| BYD-E6 | 60.0 | 280 | 21.67 |
| Average value | 47.13 | 365 | — |

With the consideration of the energy loss in actual running, the actual driving ranges are slightly smaller than the factory data. The average additional values of the battery capacities and ranges were calculated according to the proportion of each EV. In this study, it was assumed that all charging facilities on the highways were fast charging facilities, with a charging power of $P_{ch} = 96$ kW, so as to ensure that passing vehicles could be quickly charged; the initial SOC of EVs entering the highway network followed normal distribution $N(0.7, 0.01)$. The parameters of the planning model are shown in Tab. 4 and can be adjusted according to the actual situation. For instance, when K_3 is set to 0.3, the distance between two adjacent charging stations can be ensured to be no more than 58.74 km. In this example, it is ensured that there is one charging station in each of the five adjacent calculation points, and the distances are relatively appropriate.

Table 4 Parameters of the planning of the EV charging facilities in the highway network

| Parameter | Value | Parameter | Value | Parameter | Value |
|------------------|------------------|---------------|-----------------|---------------------|-----------|
| S_{down} | 0.4 | L_{max} | 0.8 | β_k^{cs} | 0.9 |
| S_{up} | 1 | α_{cs} | 0.85 | M | $1e^{10}$ |
| i | 6.8% | c_{con} | 200100 CNY / km | B^{av} | 35.21 kWh |
| s | 10 | τ | 0.7 | ΔSOC_j^{av} | 0.7 |
| c_{ch} | 21165 CNY / unit | c_p^* | 0.76/kWh | K_1 | 0.25 |
| c_{tr} | 357.29 CNY / kVA | p_{cs}^{av} | 15 kW | K_2 | 0.1 |
| K_{ch} | 0.7 | T_{cs}^{av} | 4015 h | β_1 | 0.3 |
| η_{ch} | 90% | c_{hr}^0 | 12000 CNY | K_{line} | 0.2 |
| $\cos \phi_{ch}$ | 0.95 | c_m^0 | 59.2 CNY/kVA | — | — |

5.2 EV Charging Demand Characteristics

Before planning the layout of EV charging facilities on highways, the charging demand of the example network was predicted based on the SOC demand model. It was assumed that all vehicles drove at a constant speed. Without considering the influence of acceleration and deceleration, based on the calculation results of a single highway, we superimposed the SOC changes of each vehicle to obtain the SOC of vehicles passing through the node in the statistical time period $t = 1$ h. By calculating the required power of EVs in the rechargeable interval $[0, 0.4)$, the charging demand of EVs passing through the node in the time period t can be obtained. The charging demand of EVs passing through node k in a day can be obtained by integrating all time periods t throughout the day. Considering the actual characteristics of the example highway network, as shown in the Fig. 5, there are 16 nodes

in the highway network, some of these nodes have similar characteristics, to make the analysis process more clear, we selected nodes 1, 3, 6, 9, 11, 13, 14, 15, and 16 for demand analysis. The results are shown in Fig. 6a to Fig. 6i.

In terms of time distribution, the peak charging demand is concentrated in the period of 9:00-16:00. Therefore, we analyzed the charging demand characteristics of each node in this period. Nodes 1, 3, 6, and 9 are the OD points of a single highway, the corresponding charging demand is relatively small, and the peak charging demand is 120-140; nodes 13 and 14 are the intersections of three highways, and the peak charging demand is 140-160; nodes 11, 15 and 16 are the intersections of four highways, and the peak charging demand is 170-190. Therefore, for different sections and nodes of the highway network, charging demand varies. When planning the layout of charging facilities, the charging demand of various nodes should be seriously considered.

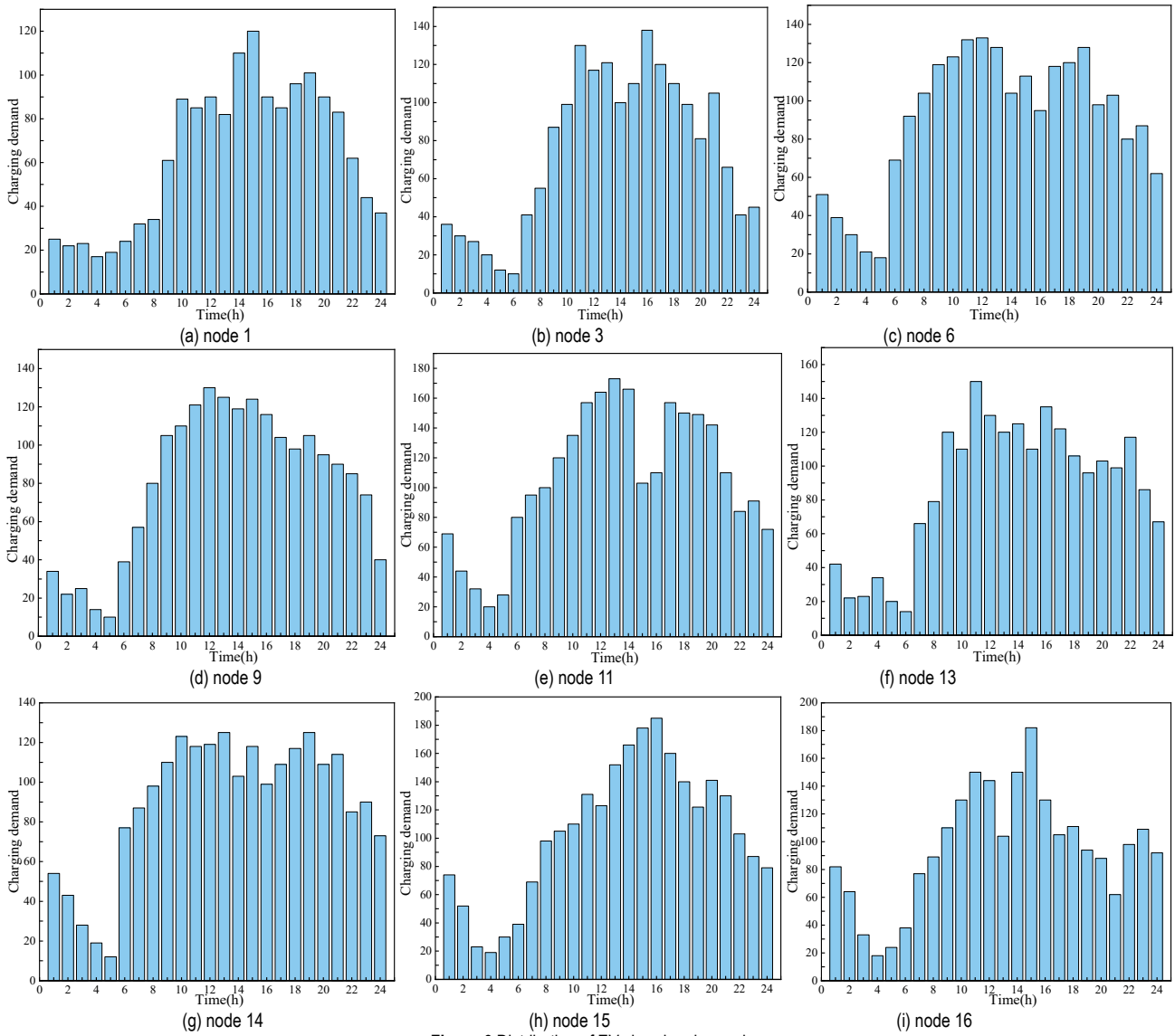


Figure 6 Distribution of EV charging demand

5.3 Layout Scheme of Charging Facilities

To improve the economy of the planning of EV charging facilities, the construction cost, grid access cost, operation and maintenance costs and the carbon emission reduction benefits generated by the planning of facilities were comprehensively considered in the objective function. Based on the established multi-objective optimization model, the CCSSA algorithm was adopted to solve the layout scheme of charging facilities. According to the characteristics of the objective function, two planning schemes were considered in this study. In Scheme 1, carbon emission reduction benefits were not considered; in

Scheme 2, carbon emission reduction benefits were considered. Candidate charging stations need to be selected at a certain interval. A smaller interval can lead to higher calculation accuracy but a greater amount of computation and higher planning difficulty. Therefore, in the layout of charging facilities, reasonable station intervals should be selected based on the charging demand characteristics of sections and nodes and the planning requirements for charging facilities.

Tab. 5 shows various costs of optimizing the locations and capacities of charging facilities at different impact factors m . A smaller value of m leads to a smaller selection range of charging stations.

Table 5 Costs of EV charging facilities on the highways

| m | $c_{EVCS}(Y, N)/10^4\text{CNY}$ | | $c_{S2G}(Y, N)/10^4\text{CNY}$ | | $C_{oper}(Y, N)/10^4\text{CNY}$ | | $C_{emf}/10^4\text{CNY}$ | |
|-----|---------------------------------|---------|--------------------------------|---------|---------------------------------|---------|--------------------------|----------|
| | Scheme1 | Scheme2 | Scheme1 | Scheme2 | Scheme1 | Scheme2 | Scheme1 | Scheme2 |
| 2 | 4546.81 | 4932.74 | 3628.11 | 3914.34 | 4013.90 | 4244.23 | -43.77 | -9020.22 |
| 3 | 5021.92 | 5329.27 | 4417.20 | 4615.62 | 4832.32 | 4957.31 | -76.15 | -9216.46 |
| 4 | 5638.11 | 5874.35 | 4092.42 | 4372.13 | 4955.43 | 5103.88 | -90.02 | -9548.31 |
| 5 | 6199.17 | 6433.39 | 4967.04 | 5016.39 | 5201.80 | 5392.02 | -65.34 | -9737.85 |
| 6 | 6547.02 | 6815.75 | 5514.82 | 5722.30 | 5642.55 | 5823.13 | -71.71 | -9893.09 |
| 7 | 7446.26 | 7672.94 | 5739.49 | 5964.75 | 5989.65 | 6032.32 | -62.56 | -9925.77 |
| 8 | 7892.13 | 7997.45 | 5987.77 | 6177.04 | 6227.76 | 6431.41 | -54.38 | -9973.04 |

With an increase in the value of m , the number of stations increases, the annual average cost of building stations increases, and the selection of charging stations is more flexible. When the charging demand can be satisfied by only one charge while users pass through multiple charging stations, it means that the charging stations are densely distributed, the risk of power shortage is low, the number of corresponding stations is excessive, and the costs of station construction are relatively high.

We calibrated the schemes at different m values and

found that as the value increased, the satisfaction rate of EVs improved; when $m = 4$, the charging demand of all types of EVs could be almost completely satisfied. Therefore, to improve the utilization rate of charging stations, ensure the economy of the planning scheme, and reduce the risk of power depletion in EVs, in this study, it was assumed that EV users charged at least once for every four charging stations they passed, i.e., $m = 4$, then $\gamma_{jk} = 1/4, \lambda_{jk} = 1/4$.

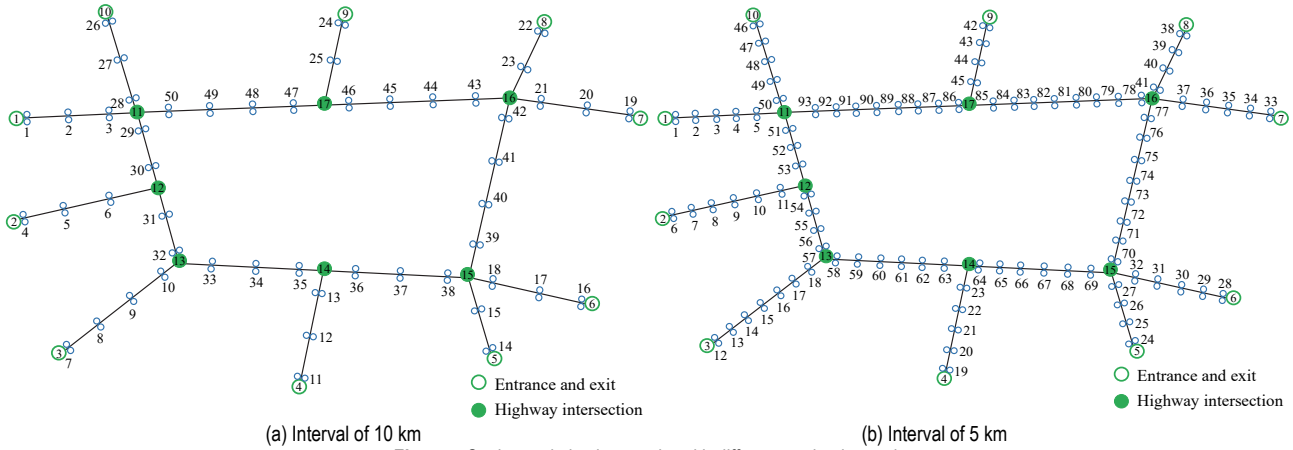


Figure 7 Station optimization results with different station intervals

Fig. 7 shows the optimization results of stations with different intervals. When carbon emission benefits are not considered, the station interval is 10 km, and the final number of stations selected is $N_c = 100$; when carbon emission benefits are considered, the station interval is 5 km, and the final number of stations selected is $N_c = 186$. The upper and lower constraints of the number of charging stations were set to 30 and 70, and the upper and lower

constraints of the charging station capacity were set to 5 and 15 chargers. The CCSSA algorithm was used to obtain the optimal locations and capacities of the planning. A total of 37 stations are built when carbon emission benefits are not considered, and 67 stations are built when carbon emission benefits are considered. The planning results of the highway network are shown in Fig. 8.

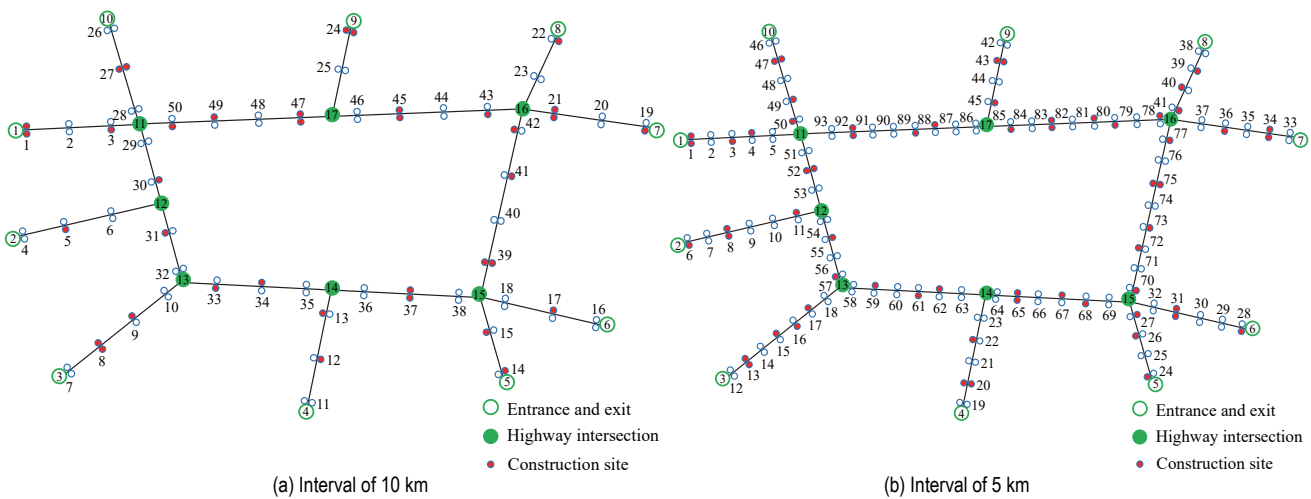


Figure 8 Layout results of charging facilities on the highways

The objective value of Scheme 1 was 164.73, and the objective function stabilized when the number of convergence iterations was 410; the objective value of Scheme 2 was 91.45, and the objective function stabilized when the number of convergence iterations was 330. The convergence curves of the two schemes are shown in Fig. 9. i_1 represents the analysis results of the CCSSA algorithm, while i_2 represents the analysis results of the CSO

algorithm. When carbon emission benefits are considered, the number of convergence iterations required for stabilization is smaller, and the value of the objective function is smaller. Therefore, the layout result with the consideration of carbon emission benefits is more reasonable. The final layout scheme of EV charging facilities in the highway network based on the CCSSA algorithm is shown in Tab. 6.

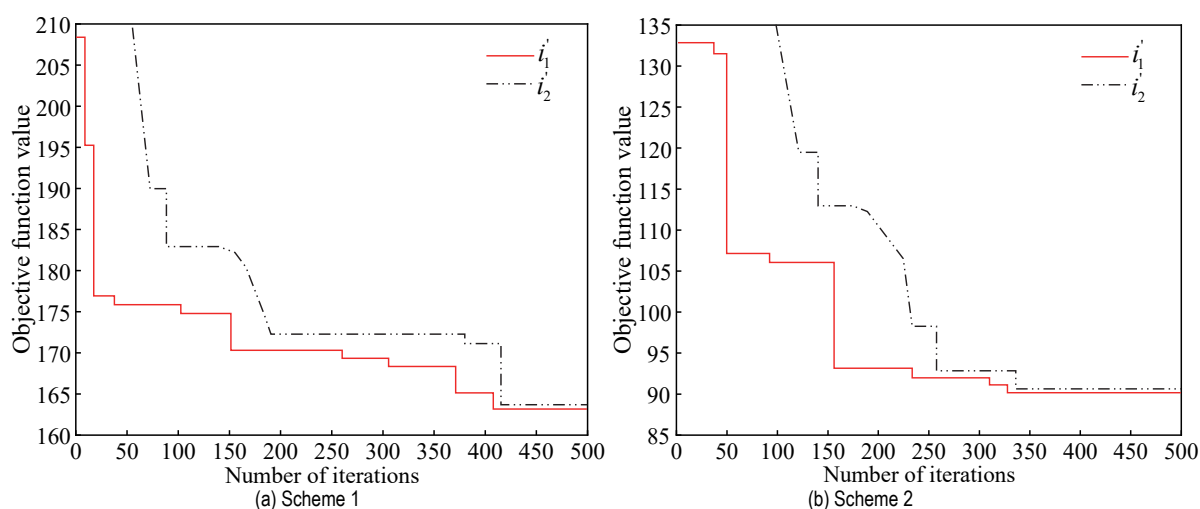


Figure 9 Convergence curves of different layout schemes

Table 6 Layout locations of the charging stations and the number of facilities

| Layout scheme | Station location | Number of piles |
|---------------|------------------|-----------------|------------------|-----------------|------------------|-----------------|------------------|-----------------|
| Scheme 1 | 1/51 | 5 | 14 | 8 | 27/77 | 8 | 41 | 6 |
| | 3 | 6 | 65 | 7 | 80 | 10 | 92 | 7 |
| | 5 | 5 | 17 | 5 | 31 | 8 | 93 | 9 |
| | 8/58 | 6 | 69 | 6 | 33 | 7 | 45/95 | 5 |
| | 59 | 7 | 21/71 | 9 | 84 | 5 | 47/97 | 10 |
| | 12 | 5 | 72 | 7 | 37/87 | 9 | 49 | 8 |
| Scheme 2 | 63 | 6 | 24/74 | 6 | 39/89 | 11 | 100 | 7 |
| | 1/94 | 8 | 117 | 6 | 47/140 | 9 | 70 | 6 |
| | 3 | 11 | 119 | 6 | 142 | 14 | 165 | 9 |
| | 98 | 10 | 27 | 8 | 50 | 11 | 73 | 10 |
| | 6 | 6 | 121 | 10 | 52/145 | 8 | 75/168 | 7 |
| | 8/101 | 7 | 31/124 | 9 | 148 | 9 | 77 | 9 |
| | 104 | 9 | 34/127 | 11 | 57 | 6 | 173 | 8 |
| | 13/106 | 6 | 129 | 9 | 152 | 5 | 81 | 6 |
| | 108 | 7 | 132 | 8 | 61 | 8 | 83/176 | 5 |
| | 16 | 8 | 40 | 9 | 155 | 8 | 178 | 13 |
| Scheme 2 | 110 | 5 | 134 | 12 | 65/158 | 9 | 88 | 11 |
| | 20/113 | 10 | 43/136 | 11 | 160 | 7 | 180 | 9 |
| | 115 | 7 | 138 | 10 | 68 | 10 | 92/185 | 10 |

5.4 Algorithm Comparison

To verify the effectiveness of the proposed CCSSA algorithm, we compared the solution results of the standard GA algorithm, CSO algorithm and CCSSA algorithm in this study. The three algorithms were used to conduct test trials on six nonlinear functions with multiple local extreme points, including the Schaffer, Shubert, Griewank, Rastrigin, Rosenbrock, and Zakharov functions. Based on the test results, we analyzed the performance of the proposed algorithm. The parameters of the algorithm were set as follows: the swarm size was set to 110, the grouping rate was 0.2, the annealing constant was 0.5, the number of cycles in the tracking mode was 3, the number of iterations was 400, and the number of dimensions was 4. Each test function was run 100 times, and the optimal solution output of the algorithm was recorded in each run. The average convergence time, average optimal solution and the standard deviation of the optimal solution were calculated for 100 runs of the algorithm. The algorithm optimization performance was measured as the average of the global optimal values of the benchmark functions.

The simulations of the six benchmark functions were performed with the same number of iterations. The results are shown in Tab. 7, and the correspondence between the

optimal values and the number of runs is shown in Fig. 10.

Table 7 Analytical results of the algorithm optimization performance under different functions

| Function | Algorithm | Average convergence time / s | Average optimal solution | Standard deviation of the optimal solution |
|------------|-----------|------------------------------|--------------------------|--|
| Schaffer | GA | 0.0228 | 0.0251 | 0.0164 |
| | CSO | 0.0177 | 0.0176 | 0.0098 |
| | CCSSA | 0.0124 | 0.0073 | 0.0013 |
| Shubert | GA | 0.1628 | -164.89 | 47.8366 |
| | CSO | 0.1413 | -197.04 | 23.1024 |
| | CCSSA | 0.1057 | -231.43 | 5.6391 |
| Griewank | GA | 0.0393 | 9.5641 | 9.3056 |
| | CSO | 0.0254 | 4.3768 | 1.6204 |
| | CCSSA | 0.0185 | 2.9012 | 1.3493 |
| Rastrigin | GA | 0.6749 | 1.3984 | 1.3872 |
| | CSO | 0.6021 | 0.2618 | 0.2815 |
| | CCSSA | 0.4988 | 0.1867 | 0.2102 |
| Rosenbrock | GA | 0.0512 | 28.992 | 33.2193 |
| | CSO | 0.0457 | 14.273 | 16.1677 |
| | CCSSA | 0.0293 | 8.135 | 5.2938 |
| Zakharov | GA | 0.0394 | 2.7301 | 9.1023 |
| | CSO | 0.0288 | 2.1279 | 5.2024 |
| | CCSSA | 0.0206 | 1.8745 | 1.0803 |

Taking the Rastrigin function as an example, the average optimal solutions of the GA, CSO, and CCSSA

algorithms are 1.3984, 0.2618, and 0.1867, respectively, the CCSSA algorithm has the smallest average optimal value, and the optimization performance of this algorithm is the best. The average convergence time of the three algorithms is 0.6749, 0.6021, and 0.4988 s, respectively, and the CCSSA algorithm has the highest average convergence speed. The standard deviations of the optimal solutions of the three algorithms are 1.3872, 0.2815, and 0.2102, respectively, and the CCSSA algorithm has the

smallest standard deviation and the highest accuracy. The optimization performance of the three algorithms shows the same trend in the experimental results of the other functions. In conclusion, compared with the GA and the standard CSO algorithms, the CCSSA algorithm has the highest convergence speed, the smallest function objective value and the most stable overall iteration curve. In addition, the CCSSA algorithm is better than the other two algorithms in terms of overall search capability.

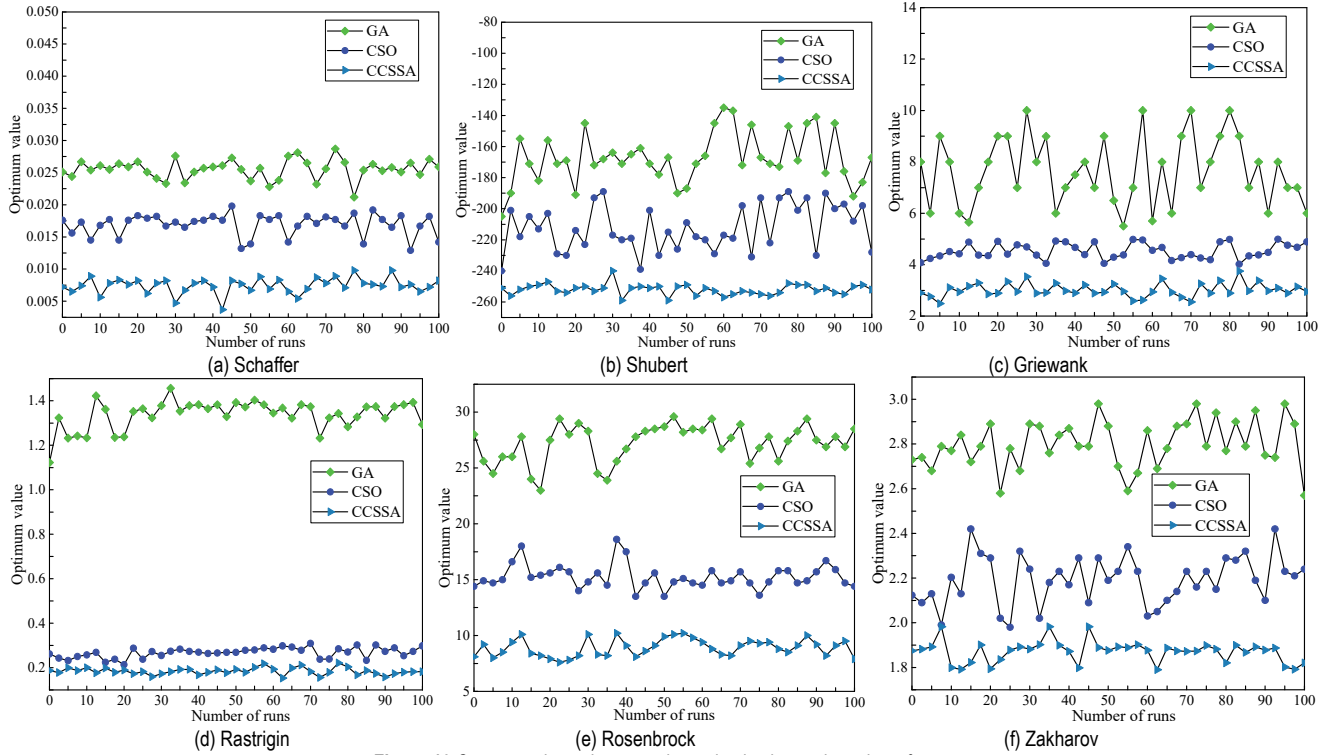


Figure 10 Correspondence between the optimal value and number of runs

6 CONCLUSION

In this study, for the layout planning of EV charging facilities on highways, based on the charging demand characteristics of EVs, we built a multi-objective optimization model with a minimum construction cost of charging facilities, a minimum grid access cost, minimum operation and maintenance costs, and maximum carbon emission reduction benefits. A CCSSA algorithm combining the CSO algorithm and simulated annealing method was proposed to optimize the layout of charging facilities. Chaotic logistic mapping was introduced into the standard CSO algorithm, changing the location information on the cat swarm during the iterative process. The simulated annealing method was adopted for global optimization search so that the whole swarm was balanced in local and global search capabilities to obtain the optimal distribution strategy of charging facilities. The case study results of the highway network in Xi’an City, Shaanxi Province, China, showed that the layout model with consideration of carbon emission reduction benefits minimized the comprehensive cost. In this layout model, the economic and environmental benefits can be taken into account. The obtained layout scheme had a reasonable station interval and met the daily charging demand in the target highway network. Moreover, the obtained target cost function value was relatively small, with a high

convergence speed and high economy. In addition, the CCSSA algorithm could effectively solve the “premature” problem of the CSO algorithm. The CCSSA algorithm was superior to the GA and standard CSO algorithms. It could better adapt to the dynamic environment and effectively track the global optimal value. It had stronger search capability and higher prediction accuracy than the other algorithms in the layout planning of facilities.

However, the proposed model and method have some limitations. Firstly, only the fast charging form was considered in the prediction of charging demand, which is not consistent with the actual charging form expected by users in different SOC states. Furthermore, in the calculation of carbon emission reduction benefits, only the carbon emission from fuel vehicles was considered, while the emission from the operation and maintenance of buildings and other activities were not taken into account. Finally, the application effect and solution accuracy of the CCSSA algorithm in uncertain environments need to be further studied. The proposed approach will be improved in the future to address the above limitations.

Acknowledgments

This research is supported by the Fundamental Research Funds for the Central Universities of China (2021YJS080), the National Natural Science Foundation of

China (71340020), and the National Social Science Fund of China (2021ZKKT014).

7 REFERENCES

- [1] Hosseini, S. & Sarder, M. D. (2019). Development of a Bayesian network model for optimal site selection of electric vehicle charging station. *International Journal of Electrical Power & Energy Systems*, 105, 110-122. <https://doi.org/10.1016/j.ijepes.2018.08.011>
- [2] Neaimeh, M., Salisbury, S. D., Hill, G. A., Blythe, P. T., Scoffield, D. R., & Francfort, J. E. (2017). Analysing the usage and evidencing the importance of fast chargers for the adoption of battery electric vehicles. *Energy Policy*, 108, 474-486. <https://doi.org/10.1016/j.enpol.2017.06.033>
- [3] Yang, S. N., Cheng, W. S., Hsu, Y. C., Gan, C. H., & Lin, Y. B. (2013). Charge scheduling of electric vehicles in highways. *Mathematical and Computer Modelling*, 57(11), 2873-2882. <https://doi.org/10.1016/j.mcm.2011.11.054>
- [4] Liu, J.-Y., Liu, S.-F., & Gong, D.-Q. (2021). Electric Vehicle Charging Station Layout Based on Particle Swarm Simulation. *International Journal of Simulation Modelling*, 20(4), 754-765. <https://doi.org/10.2507/IJSIMM20-4-CO17>
- [5] Bae, S. & Kwasinski, A. (2012). Spatial and Temporal Model of Electric Vehicle Charging Demand. *IEEE Transactions on Smart Grid*, 3(1), 394-403. <https://doi.org/10.1109/TSG.2011.2159278>
- [6] Wager, G., Whale, J., & Braunl, T. (2016). Driving electric vehicles at highway speeds: The effect of higher driving speeds on energy consumption and driving range for electric vehicles in Australia. *Renewable and Sustainable Energy Reviews*, 63, 158-165. <https://doi.org/10.1016/j.rser.2016.05.060>
- [7] Mullan, J., Harries, D., Bräunl, T., & Whitely, S. (2011). Modelling the impacts of electric vehicle recharging on the Western Australian electricity supply system. *Energy Policy*, 39(7), 4349-4359. <https://doi.org/10.1016/j.enpol.2011.04.052>
- [8] Huiyi, W., Xueliang, H., Lixin, C., & Yuqi, Z. (2015). Highway electric vehicle charging load prediction and its impact on the grid. *Proceedings of the 2015 2nd International Forum on Electrical Engineering and Automation (IFEEA 2015)*. <https://doi.org/10.1016/j.ifeea.2015.09.021>
- [9] Marmaras, C., Xydias, E., & Cipcigan, L. (2017). Simulation of electric vehicle driver behaviour in road transport and electric power networks. *Transportation Research Part C: Emerging Technologies*, 80, 239-256. <https://doi.org/10.1016/j.trc.2017.05.004>
- [10] Ferrero, E., Alessandrini, S., & Balanzino, A. (2016). Impact of the electric vehicles on the air pollution from a highway. *Applied Energy*, 169, 450-459. <https://doi.org/10.1016/j.apenergy.2016.01.098>
- [11] Zhu, Z. H., Gao, Z. Y., Zheng, J. F., & Du, H. M. (2016). Charging station location problem of plug-in electric vehicles. *Journal of Transport Geography*, 52, 11-22. <https://doi.org/10.1016/j.jtrangeo.2016.02.002>
- [12] Chandra Mouli, G.R., Bauer, P., & Zeman, M. (2016). System design for a solar powered electric vehicle charging station for workplaces. *Applied Energy*, 168, 434-443. <https://doi.org/10.1016/j.apenergy.2016.01.110>
- [13] Sun, X. H., Yamamoto, T., & Morikawa, T. (2016). Fast-charging station choice behavior among battery electric vehicle users. *Transportation Research Part D: Transport and Environment*, 46, 26-39. <https://doi.org/10.1016/j.trd.2016.03.008>
- [14] Arslan, O., Yıldız, B., & Ekin Kardeş, O. (2014). Impacts of battery characteristics, driver preferences and road network features on travel costs of a plug-in hybrid electric vehicle (PHEV) for long-distance trips. *Energy Policy*, 74, 168-178. <https://doi.org/10.1016/j.enpol.2014.08.015>
- [15] Sun, Z., Gao, W., Li, B., & Wang, L. (2020). Locating charging stations for electric vehicles. *Transport Policy*, 98, 48-54. <https://doi.org/10.1016/j.tranpol.2018.07.009>
- [16] Tian, Z., Hou, W., Gu, X., Gu, F., & Yao, B. (2018). The location optimization of electric vehicle charging stations considering charging behavior. *Simulation*, 94(7), 625-636. <https://doi.org/10.1177/0037549717743807>
- [17] Liu, D. & Ge, Y. E. (2018). Modeling assignment of quay cranes using queueing theory for minimizing CO₂ emission at a container terminal. *Transportation Research Part D: Transport and Environment*, 61, 140-151. <https://doi.org/10.1016/j.trd.2017.06.006>
- [18] Yang, Y., Tian, N., Wang, Y., & Yuan, Z. (2022). A parallel FP-Growth mining algorithm with load balancing constraints for traffic crash data. *International Journal of Computers Communications & Control*, 17(4), 4806. <https://doi.org/10.21203/rs.3.rs-1311180/v1>
- [19] Zhang, L., Brown, T., & Samuelsen, S. (2013). Evaluation of charging infrastructure requirements and operating costs for plug-in electric vehicles. *Journal of Power Sources*, 240, 515-524. <https://doi.org/10.1016/j.jpowsour.2013.04.048>
- [20] Noori, M., Gardner, S., & Tatari, O. (2015). Electric vehicle cost, emissions, and water footprint in the United States: Development of a regional optimization model. *Energy*, 89, 610-625. <https://doi.org/10.1016/j.energy.2015.05.152>
- [21] Dong, X., Mu, Y., Jia, H., Wu, J., & Yu, X. (2016). Planning of Fast EV Charging Stations on a Round Freeway. *IEEE Transactions on Sustainable Energy*, 7(4), 1452-1461. <https://doi.org/10.1109/tste.2016.2547891>
- [22] Yang, Y., Yang, B., Yuan, Z., Meng, R., & Wang, Y. (2023). Modelling and comparing two modes of sharing parking spots at residential area: Real-time and fixed-time allocation. *IEEE Intelligent Transport Systems*, 1-20. <https://doi.org/10.1049/itr2.12343>
- [23] Pereira, J. & Averbakh, I. (2011). Exact and heuristic algorithms for the interval data robust assignment problem. *Computers & Operations Research*, 38(8), 1153-1163. <https://doi.org/10.1016/j.cor.2010.11.009>
- [24] Ang, B. W. & Liu, F. L. (2001). A new energy decomposition method: perfect in decomposition and consistent in aggregation. *Energy*, 26(6), 537-548. [https://doi.org/10.1016/S0360-5442\(01\)00022-6](https://doi.org/10.1016/S0360-5442(01)00022-6)
- [25] Altay, N., Robinson, P. E., & Bretthauer, K. M. (2008). Exact and heuristic solution approaches for the mixed integer setup knapsack problem. *European Journal of Operational Research*, 190(3), 598-609. <https://doi.org/10.1016/j.ejor.2007.07.003>
- [26] Yang, Y., Yuan, Z., Chen, J., & Guo, M. (2017). Assessment of osculating value method based on entropy weight to transportation energy conservation and emission reduction. *Environment Engineering & Management Journal*, 16(10), 2413-2423. <https://doi.org/10.30638/eemj.2017.249>
- [27] Zografos, K. G. & Androutsopoulos, K. N. (2004). A heuristic algorithm for solving hazardous materials distribution problems. *European Journal of Operational Research*, 152(2), 507-519. [https://doi.org/10.1016/S0377-2217\(03\)00041-9](https://doi.org/10.1016/S0377-2217(03)00041-9)
- [28] Marini, F. & Walczak, B. (2015). Particle swarm optimization (PSO). A tutorial. *Chemometrics and Intelligent Laboratory Systems*, 149, 153-165. <https://doi.org/10.1016/j.chemolab.2015.08.020>
- [29] Wu, X., Bai, W., Xie, Y., Sun, X., Deng, C., & Cui, H. (2018). A hybrid algorithm of particle swarm optimization, metropolis criterion and RTS smoother for path planning of UAVs. *Applied Soft Computing*, 73, 735-747. <https://doi.org/10.1016/j.asoc.2018.09.011>
- [30] Zheng, W., Ren, P., Ge, P., Qiu, Y., & Liu, Z. (2012). Hybrid heuristic algorithm for two-dimensional steel coil cutting problem. *Computers & Industrial Engineering*, 62(3), 829-

838. <https://doi.org/10.1016/j.cie.2011.12.012>
- [31] Moussavi, S. E., Mahdjoub, M., & Grunder, O. (2018). A hybrid heuristic algorithm for the sequencing generalized assignment problem in an assembly line. *IFAC-Papers online*, 51(2), 695-700.
<https://doi.org/10.1016/j.ifacol.2018.03.118>
- [32] Rautray, R. & Balabantaray, R. C. (2017). Cat swarm optimization based evolutionary framework for multi document summarization. *Physica A: Statistical Mechanics and its Applications*, 477, 174-186.
<https://doi.org/10.1016/j.physa.2017.02.056>
- [33] Pappula, L. & Ghosh, D. (2018). Cat swarm optimization with normal mutation for fast convergence of multimodal functions. *Applied Soft Computing*, 66, 473-491.
<https://doi.org/10.1016/j.asoc.2018.02.012>
- [34] Pradhan, P. M. & Panda, G. (2012). Solving multiobjective problems using cat swarm optimization. *Expert Systems with Applications*, 39(3), 2956-2964.
<https://doi.org/10.1016/j.eswa.2011.08.157>
- [35] Liu, J., Huang, T., Chen, J., & Liu, Y. (2011). A new algorithm based on the proximity principle for the virtual network embedding problem. *Journal of Zhejiang University SCIENCE C*, 12(11), 910.
<https://doi.org/10.1631/jzus.C1100003>

Contact information:**Qingqiao GENG**

Transport Planning and Research Institute,
Ministry of Transport, Beijing 100028, China
E-mail: 20114066@bjtu.edu.cn

Dongye SUN

China Transport Telecommunications & Information Center,
No. 1 Houshen, Anwai Waiguan, Chaoyang District, Beijing 100011, P. R. China
E-mail: sundongye@cttic.cn

Yuanhua JIA

(Corresponding author)
School of Traffic and Transportation,
Beijing Jiaotong University,
No. 3 Shangyuancun, Haidian District, Beijing 100044, P. R. China
E-mail: yhjia@bjtu.edu.cn